

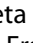












## MICA/B-targeted antibody promotes NK cell-driven tumor immunity in patients with intrahepatic cholangiocarcinoma

Barbara Oliviero <sup>a</sup>, Stefania Varchetta <sup>a</sup>, Dalila Mele <sup>a</sup>, Greta Pessino <sup>a</sup>, Roberta Maiello <sup>b</sup>, Monica Falleni<sup>c</sup>, Delfina Tosi<sup>c</sup>, Matteo Donadon<sup>d</sup>, Cristiana Soldani <sup>d</sup>, Barbara Franceschini<sup>d</sup>, Guido Torzilli<sup>d</sup>, Gaetano Piccolo <sup>e</sup>, Matteo Barabino <sup>e</sup>, Enrico Opocher <sup>e</sup>, Marcello Maestri <sup>f</sup>, Stefano Bernuzzi <sup>g</sup>, Kai W. Wucherpfnig<sup>h</sup>, Mario U. Mondelli <sup>a,i</sup>, and Stefania Mantovani <sup>a</sup>

<sup>a</sup>Division of Clinical Immunology - Infectious Diseases, Department of Medicine, Fondazione IRCCS Policlinico San Matteo, Pavia, Italy; <sup>b</sup>Department of Molecular Medicine, University of Pavia, Pavia, Italy; <sup>c</sup>Department of Pathology, Department of Health Sciences, ASST Santi Paolo e Carlo, State University of Milan, Milan, Italy; <sup>d</sup>Department of Hepatobiliary and General Surgery, Humanitas Clinical and Research Center, Humanitas University, Rozzano, Italy; <sup>e</sup>Division of Gastrointestinal Surgery, ASST Santi Paolo e Carlo, and State University of Milan, Milan, Italy; <sup>f</sup>Division of General Surgery 1, Department of Surgery, Fondazione IRCCS Policlinico San Matteo, Pavia, Italy; <sup>g</sup>Immunohematology and Transfusion Service, Department of Diagnostic Medicine, Fondazione IRCCS Policlinico San Matteo, Pavia, Italy; <sup>h</sup>Department of Cancer Immunology and Virology, Dana-Farber Cancer Institute, Boston, Massachusetts, USA; <sup>i</sup>Department of Internal Medicine and Therapeutics, University of Pavia, Pavia, Italy

### ABSTRACT

The major histocompatibility complex-class I chain related proteins A and B (MICA/B) is upregulated because of cellular stress and MICA/B shedding by cancer cells causes escape from NKG2D recognition favoring the emergence of cancers. Cholangiocarcinoma (CCA) is a relatively rare, though increasingly prevalent, primary liver cancer characterized by a late clinical presentation and a dismal prognosis. We explored the NKG2D-MICA/B axis in NK cells from 41 patients with intrahepatic cholangiocarcinoma (iCCA). The MICA/B-specific 7C6 mAb was used for *ex vivo* antibody-dependent cytotoxicity (ADCC) experiments using circulating, non tumor liver- and tumor-infiltrating NK cells against the HuCCT-1 cell line and patient-derived primary iCCA cells as targets. MICA/B were more expressed in iCCA than in non-tumoral tissue, MICA transcription being higher in moderately-differentiated compared with poorly-differentiated cancer. Serum MICA was elevated in iCCA patients in line with higher expression of ADAM10 and ADAM17 that are responsible for proteolytic release of MICA/B from tumor. Addition of 7C6 significantly boosted peripheral, liver- and tumor-infiltrating-NK cell degranulation and IFN $\gamma$  production toward MICA/B-expressing established cell lines and autologous iCCA patient target cells. Our data show that anti-MICA/B drives NK cell anti-tumor activity, and provide preclinical evidence in support of 7C6 as a potential immunotherapeutic tool for iCCA.

### ARTICLE HISTORY

Received 7 September 2021  
Revised 25 January 2022  
Accepted 26 January 2022

### KEYWORDS



Natural killer cells; liver cancer; innate immunity; ADCC; immunotherapy

## Introduction

Cholangiocarcinoma (CCA) is a heterogeneous group of malignant tumors that originate from the biliary tree. Depending on the anatomical location, CCA is classified as intrahepatic (iCCA), perihilar (pCCA) and distal (dCCA). pCCA accounts for approximately 50–60% of all CCA, followed by dCCA (20–30%) and iCCA (10–20%). CCA is the second most common primary hepatic malignancy after hepatocellular carcinoma (HCC), accounting for approximately 15% of all primary liver tumors and 3% of gastrointestinal cancers. Although CCA is a rare cancer (<3 per 100,000 person-years), its incidence is exceptionally high in some countries where the liver fluke *Opisthorchis viverrini* is endemic.<sup>1–3</sup>

In contrast to HCC which virtually always arises in the background of cirrhosis, CCA mostly develops within a normal liver. CCA is usually asymptomatic in early stages and nearly two-thirds of patients have metastatic or locally advanced disease at diagnosis, when potentially curative

treatments such as surgical resection or liver transplantation cannot be applied, resulting in a dismal prognosis.<sup>4</sup> Chemotherapy with cisplatin plus gemcitabine still represents the mainstay of treatment for patients with advanced CCA.<sup>5</sup> However, given the modest efficacy of this regimen, additional cytotoxic agents and combinations have been used as second-line chemotherapy but no clear benefit has been shown.<sup>6</sup> Therefore, there is a pressing medical need to discover new effective agents and/or to develop additional therapeutic approaches. Immunotherapy includes immune checkpoint inhibitors (ICI), targeting mainly programmed death 1 (PD-1) and PD-ligand1 (PD-L1), cancer vaccines, and adoptive cell transfer. Pembrolizumab, a PD-1 inhibitor, demonstrated an objective response rate (ORR) of 13% in patients affected by biliary tract cancer (BTC) in the phase Ib basket trial KEYNOTE 028 (NCT02054806).<sup>7</sup> However, the phase II basket trial of pembrolizumab (KEYNOTE-158) in BTC patients, including CCA, failed to confirm such activity with an ORR only 5.8%, regardless of PD-L1 expression. Stratification of

**CONTACT** Mario U. Mondelli  [mario.mondelli@unipv.it](mailto:mario.mondelli@unipv.it)  UOC Immunologia Clinica – Malattie Infettive, Fondazione IRCCS Policlinico San Matteo, Viale Golgi 19, Pavia 27100, Italy

 Supplemental data for this article can be accessed on the [publisher's website](#)

© 2022 The Author(s). Published with license by Taylor & Francis Group, LLC.

This is an Open Access article distributed under the terms of the Creative Commons Attribution-NonCommercial License (<http://creativecommons.org/licenses/by-nc/4.0/>), which permits unrestricted non-commercial use, distribution, and reproduction in any medium, provided the original work is properly cited.

these patients into two groups according to PD-L1 expression showed a small increase in ORR in the PD-L1-high group.<sup>7</sup> Nivolumab, another PD-1 inhibitor, was assessed as monotherapy in two phase 1 and 2 clinical trials for advanced refractory BTC demonstrating a modest efficacy (ORR 3.3% and 11%, respectively) (NCT02829918).<sup>8,9</sup> Furthermore, several clinical trials assessed the combination of ICI with targeted therapy, local ablative therapy and chemotherapy (reviewed in<sup>10</sup>). Of note, nivolumab in combination with gemcitabine/cisplatin, appears to offer promising efficacy and a manageable safety profile for patients with unresectable or metastatic BTC, as assessed in a phase 2 trial showing an ORR of 55.6% (NCT03311789).<sup>11</sup> Moreover, combined treatment with pembrolizumab plus an antiangiogenic agent, such as ramucirumab or lenvatinib, was assessed in two studies<sup>12,13</sup> which recruited previously treated advanced BTC patients, providing ORR of 4% and 25%, respectively (NCT02443324, NCT03895970). Emerging immunological treatment strategies include adoptive immunotherapies with chimeric antigen receptor (CAR) T-cells. Ongoing clinical trials in BTC, comprising CCA, include the administration of anti-GPC3 CAR-T cells (NCT04951141), anti-EGFR CAR T cells, MUC-1 CAR-T cells (NCT03633773). A phase I study (NCT01869166) using EGFR-specific CAR T cells for EGFR-positive advanced unresectable, relapsed/metastatic BTC, including 14 CCA, showed encouraging results, with 5.8% of the patients achieving a complete response and 58.8% maintaining stable disease.<sup>14</sup>

Natural Killer (NK) cells and cytotoxic T lymphocytes represent the most relevant effector cells mediating tumor cell elimination via cytolytic activity and cytokine secretion.<sup>15</sup> NK cells express activating receptors, including the NK group 2 member D (NKG2D) receptor, which recognizes ligands displayed on the surface of cells stressed as a result of viral infection or malignant transformation. NK-mediated target cell lysis occurs through reduced expression of inhibitory signals and a simultaneously increased expression of activating signals required for NK cell triggering.<sup>16</sup> In humans, NKG2D ligands (NKG2DL) include major histocompatibility complex (MHC) class I polypeptide-related sequence A (MICA), MHC class I polypeptide-related sequence B (MICB) and the unique long 16 (UL-16)-binding proteins (ULBPs).<sup>17,18</sup> Expression of NKG2DL has been observed in hematopoietic malignancies and in a variety of solid tumors such as colorectal, ovarian, cervical, breast, pancreatic, melanoma, gastric cancers and HCC.<sup>19–27</sup> So far, only one study has investigated the expression of NKG2DL on extrahepatic CCA<sup>28</sup> showing that high expression of MICA/B correlated with overall and disease-free survival. However, MICA/B proteins are frequently downregulated by tumor cells via post-translational modifications in which the external domains of MICA/B are proteolytically cleaved by surface proteases and shed into the extracellular environment. Notably, multiple metalloproteases have been shown to cleave MICA/B, including the membrane type matrix metalloproteinase 14 (MMP14), a disintegrin and metalloproteinase 10 and 17 (ADAM10 and ADAM17 respectively).<sup>29–32</sup> Furthermore, soluble MICA and MICB that might block NKG2D receptor interaction with its cellular ligands are found in the sera of cancer patients, which frequently correlate with poor prognosis and impaired T and NK cell function.<sup>19,28</sup>

Recently, Ferrari de Andrade et al. reported an innovative approach to inhibit MICA/B cleavage via construction of a monoclonal antibody (mAb), named 7C6, that specifically bound the MICA/B  $\alpha$ -3 domain, the site where the endoplasmic reticulum protein 5 (ERp5) binds to enable subsequent cleavage.<sup>33</sup> The use of 7C6, a mAb that does not compete for binding to the NKG2D receptor, preserves the expression of MICA and MICB on tumor cells and permits NKG2D-dependent activation of NK cell effectors. Additionally, the Fc portion of 7C6 can mediate antibody-dependent cellular cytotoxicity (ADCC), triggering target-cell killing by NK cells. Moreover, the FDA-approved histone deacetylase inhibitor panobinostat and 7C6 mAb synergistically acted to enhance MICA/B surface expression on tumor cells and reduced the number of pulmonary metastases of cytotoxic T cell-resistant human melanoma cells in NOD/SCID gamma mice reconstituted with human NK cells.<sup>34</sup> Importantly, the same group showed that 7C6-mediated inhibition of MICA/B shedding promoted macrophage-driven immunity against acute myeloid leukemia via Fc receptor signaling and that the epigenetic regulator romidepsin synergized with 7C6 to upregulate MICA/B expression.<sup>35</sup> Moreover, a recent study found that the combination of cytokine-induced killer cells with 7C6 mAb enhanced degranulation and IFN $\gamma$  production against different tumor cells.<sup>36</sup> Thus, the wealth of information supporting a role for the NKG2D/MICA/B axis as a potential target in cancer immunotherapy prompted us to explore on one side MICA/B expression in iCCA tissue and on the other the use of 7C6 as a possible driver for anti-MICA/B-directed NK-cell cytotoxicity.

## Materials and methods

### Study subjects

Peripheral blood mononuclear cells (PBMC) and surgically resected iCCA specimens along with matched, non-tumoral (NT) tissue from a non-adjacent liver site were obtained from treatment-naïve patients only at Fondazione IRCCS Policlinico San Matteo, Pavia, IRCCS Humanitas Research Hospital and at ASST Santi Paolo e Carlo Hospital, Milan, Italy. Tissue samples were stored in tissue storage solution (Miltenyi Biotec, Bergisch Gladbach, Germany) or RNA later (Sigma-Aldrich, St. Louis, MO, USA). Patient characteristics are listed in [Table 1](#). Healthy controls (HC) were 19 females and 46 males, with a median age of 68 years (range 40–81 years). A written informed consent was obtained from each individual. The study protocol is compliant with the ethical guidelines of the 1975 Declaration of Helsinki and was approved by our institutional ethical committee (protocol number: P-20140031379, P-20190104922).

### Phenotypic and functional analysis

Liver-infiltrating lymphocytes (LIL) and tumor-infiltrating lymphocytes (TIL) were obtained as previously described.<sup>37</sup> Briefly, tissue samples were treated by enzymatic and mechanical dissociation with the human Tumor Dissociation Kit by gentleMACS Dissociator, according to the manufacturer's

**Table 1.** Characteristics of patients.

|                                       | iCCA       | %         |
|---------------------------------------|------------|-----------|
| Number of patients                    | 41         | -         |
| Female/Male                           | 18/23      | 44/56     |
| Median age (years) – range            | 71 (47–86) | -         |
| Cirrhosis: yes/not; na                | 3/36; 2    | 7/88; 5   |
| Vascular invasion: yes/not; na        | 18/14; 9   | 44/34; 22 |
| Perineural invasion: yes/not; na      | 7/26; 8    | 17/63; 20 |
| Lymph node status: N0                 | 27         | 66        |
| N1                                    | 7          | 17        |
| Nx                                    | 3          | 7         |
| na                                    | 4          | 10        |
| Number of tumors: single/multiple; na | 19/20; 2   | 46/49; 5  |
| Tumor size: <2 cm                     | 2          | 5         |
| 2–5 cm                                | 13         | 32        |
| >5 cm                                 | 22         | 53        |
| na                                    | 4          | 10        |
| Tumor stage: T1                       | 14         | 34        |
| T2                                    | 23         | 56        |
| T3                                    | 3          | 7         |
| T4                                    | 1          | 3         |
| Tumor grade: G1                       | 3          | 7         |
| G2                                    | 16         | 39        |
| G3                                    | 21         | 51        |
| na                                    | 1          | 3         |
| <b>Etiology</b>                       |            |           |
| HBV                                   | 4          | 10        |
| HCV                                   | 3          | 7         |
| NASH                                  | 6          | 14        |
| NAFLD                                 | 0          | 0         |
| PSC                                   | 0          | 0         |
| Alcohol abuse                         | 1          | 3         |
| Unknown                               | 27         | 66        |

na, not available; G1, well differentiated; G2, moderately differentiated; G3, poorly differentiated; HBV, hepatitis B virus; HCV, hepatitis C virus; NASH, nonalcoholic steatohepatitis; NAFLD, Nonalcoholic Fatty Liver Disease; PSC, Primary sclerosing cholangitis.

instructions (Miltenyi Biotec). The cell suspension was filtered in a 70 µm cell strainer and centrifuged twice at 50 g for 2 min to obtain LIL and TIL cells. The supernatant containing lymphocytes was washed and cryopreserved in liquid N<sub>2</sub>. To establish *in-vitro* primary tumor cell cultures, the cell pellet was plated in tissue culture flasks (Corning, NY, USA) with Dulbecco's Modified Eagle Medium (Thermo Fisher Scientific, Waltham, MA, USA) supplemented with 10% fetal bovine serum (FBS, HyClone, GE Healthcare, South Logan, Utah, USA), 1% antibiotic antimycotic solution (100 U/ml penicillin, 0.1 µg/ml streptomycin, 0.25 µg/ml amphotericin B) (Sigma-Aldrich) and 1% non-essential amino acids (Thermo Fisher Scientific). Surface expression of MICA/B, and ULBP1, ULBP2/5/6, ULBP4, as well as cytokeratin 19 (CK19) intracellular staining were examined by flow cytometry on patient-derived tumor cells and the HuCCT-1 cell line (kindly provided by professor M. Cadamuro, Dept. of Molecular Medicine, University of Padua, Italy). PBMC isolation was performed as previously described.<sup>37</sup> Flow cytometry analysis of unstimulated or IL15-stimulated cells (20 ng/ml for 15 h; Peprotech, London, UK) was performed using a 12-color FACSCelesta (BD Biosciences, San Diego, CA, USA) instrument. The fluorochrome-conjugated anti-human monoclonal antibodies (mAbs) used are listed in supplementary table 1. LIVE/DEAD® Fixable Near-IR Dead Cell Stain Kit (Thermo Fisher Scientific) was used to determine cell viability. Briefly, 3 × 10<sup>5</sup> cells were stained for surface markers with mAbs for

30 min at 4°C. Cells were subsequently fixed with BD Cytofix/Cytoperm (Becton Dickinson) and permeabilized with the BD Perm/Wash buffer (Becton Dickinson) in the presence of mAbs according to the manufacturer's instructions. For ADCC assay, patient-derived tumor cell lines or HuCCT-1 cells were cultured (5 × 10<sup>4</sup> per well) with IL15-stimulated effector cells (2.5 × 10<sup>5</sup> PBMC, 2.5 × 10<sup>5</sup> NK cells, 5 × 10<sup>5</sup> LIL or 5 × 10<sup>5</sup> TIL) in the presence of anti-CD107a and BD GolgiPlug™ Protein Transport Inhibitor (Becton Dickinson). The recombinant human IgG1 Fc (BioXcell, Lebanon, NH, USA) and the humanized anti-MICA/B 7C6-IgG1 mAb were added at a final concentration of 10 µg/ml. Samples were incubated at 37°C for 4 h followed by flow cytometry analysis. LIVE/DEAD® Fixable Near-IR Dead Cell Stain Kit (Thermo Fisher Scientific) was used to determine cell viability. Patient PB-, LIL- and TIL-NK cells originating from the same patient were tested against autologous tumor cells as targets in the ADCC assays. To enhance MICA/B expression, HuCCT-1 and patient-derived tumor cells were plated at 2.5 × 10<sup>4</sup> cells for 48 h in the presence of 10 µg/ml 7C6 mAb, a mutant 7C6 mAb and IgG1-Fc. Spontaneous NK cell degranulation and IFN $\gamma$  production were evaluated in PBMC (2.5 × 10<sup>5</sup> cells) cultured with mutant 7C6- and isotype-pretreated HuCCT-1 cells for 4 h in the presence of anti-CD107a and BD GolgiPlug™ Protein Transport Inhibitor (Becton Dickinson). For ADCC assay, 7C6- and isotype-pretreated HuCCT-1 cells were cultured with PBMC (2.5 × 10<sup>5</sup> cells) for 4 h in the presence of 7C6 mAb, anti-CD107a and BD GolgiPlug™ Protein Transport Inhibitor (Becton Dickinson). Data analysis was performed with the Kaluza 2.1 software (Beckman Coulter).

### NK cell isolation

PBMC from HC were stained for 30 min at 4°C with CD3BV421 and CD56BB700 (BD Biosciences) and subsequently were fluorescence-activated cell sorting (FACS)-sorted with FACS Aria III (BD Biosciences). LIVE/DEAD® Fixable Near-IR Dead Cell Stain Kit (Thermo Fisher Scientific) was used according to the manufacturer's instructions to determine cell viability. Sorted NK cells exhibited a purity >98%. In a second experiment, NK cells were enriched by immunomagnetic negative selection from freshly PBMC using the EasySep™ Human NK Cell Isolation kit according to the manufacturer's instructions (STEMCELL Technologies, Vancouver, Canada). In this case, NK cell purity was >95% (data not shown).

### Cytotoxicity assay

PBMC from HC and iCCA patients, LIL and TIL (5 × 10<sup>5</sup> cells) were cultured with target cells (autologous patient-derived tumor cells and HuCCT-1 cells) previously stained with carboxyfluorescein succinimidyl ester (CFSE) according to the manufacturer's instructions (Thermo Fisher Scientific) at an effector:target ratio of 10:1. The recombinant human IgG1 Fc (BioXcell) or 7C6 mAb were added to the culture at 10 µg/ml. After 24 h at 37°C, supernatant and target cells were harvested and stained according to the manufacturer's instructions with



LIVE/DEAD® Fixable Near-IR Dead Cell Stain Kit to determine cell viability (Thermo Fisher Scientific). Spontaneous target cell death was determined as frequency of CFSE+LIVE/DEAD+ cells into the wells in the absence of effector cells. Effector-induced target cell death was determined as frequency of CFSE+LIVE/DEAD+ cells in the presence of effector cells after subtracting spontaneous target cell death.

### Immunohistochemistry

Immunohistochemistry was performed on formalin-fixed paraffin-embedded tissue blocks of iCCA and NT tissue, retrieved from pathology archives. Serial 3 µm tissue sections were explored by immunohistochemistry with the automatic immunostainer DAKO OMNIS (DAKO, Glostrup, Denmark) for the expression of MICA/B, ADAM10 and ADAM17 proteins using the antibodies listed in supplementary table 1. Paraffin Tissue Section of human adult normal liver (HL) were used as control (CliniSciences, Nanterre, France). Immunohistochemical controls were run by omitting the primary antibody. For each case, the intensity of immunoreactivity for MICA/B, ADAM10 and ADAM17 proteins (0: negative; 1: mild, 2: medium and 3: strong) and the percentage of tumor parenchyma involved (0: negative; 1: <50% and 2: >50%) were evaluated, as reported in supplementary table 2.

### RNA extraction, qPCR and ddPCR

Tissue RNA extraction and cDNA synthesis were performed as previously described.<sup>37</sup> The SsoAdvanced Universal SYBR Green Supermix (BioRad, Hercules, CA, USA) was used and qPCR data were analyzed using the  $2^{-\Delta C_t}$  method. MICA mRNA expression was normalized to glyceraldehyde 3-phosphate dehydrogenase gene (GAPDH). The following primers were used: GAPDH forward 5'-CGGATTTGGTCGTATTGG-3' and reverse 5'-GGTGGAAATCATATTGGAACA-3'; MICA forward 5'-TCCTGCTTCTGGCTGGCAT-3' and reverse 5'-GACAGCACCGTGAGGTTA-3' (Primm, Milan, Italy). The digital droplet PCR (ddPCR) was performed with the ddPCR™ Supermix for probes with the following primers: TBP dHsaCPE5058363, ADAM10 dHsaCPE502553, ADAM17 dHsaCPE5038420 (Bio-Rad). The total mix was placed into the 8 channel cartridge and the droplets were generated with the QX200™ droplet generator (Bio-Rad). Droplets were transferred to an Eppendorf® 96 well plate (Eppendorf, Germany) and placed into the T100™ Thermal Cycler (Bio-Rad) according to the manufacturer's instructions. The droplets were subsequently read automatically by the QX200™ droplet reader (Bio-Rad) and the data were analyzed with the QuantaSoft™ analysis PRO version1 software (Bio-Rad).

### ELISA

Serum levels of soluble MICA (sMICA) were measured by a Human ELISA kit (Abcam, ab100592) in patients and HC, according to the manufacturer's instructions.

### Statistical analysis

This was performed using the GraphPad Prism 8.4.3 software (GraphPad, La Jolla, CA, USA). Data distributions among groups were checked for normality prior to any analysis. We used parametric and non-parametric tests for our analyses that are detailed in figures' legend. A p value ≤.05 was deemed statistically significant.

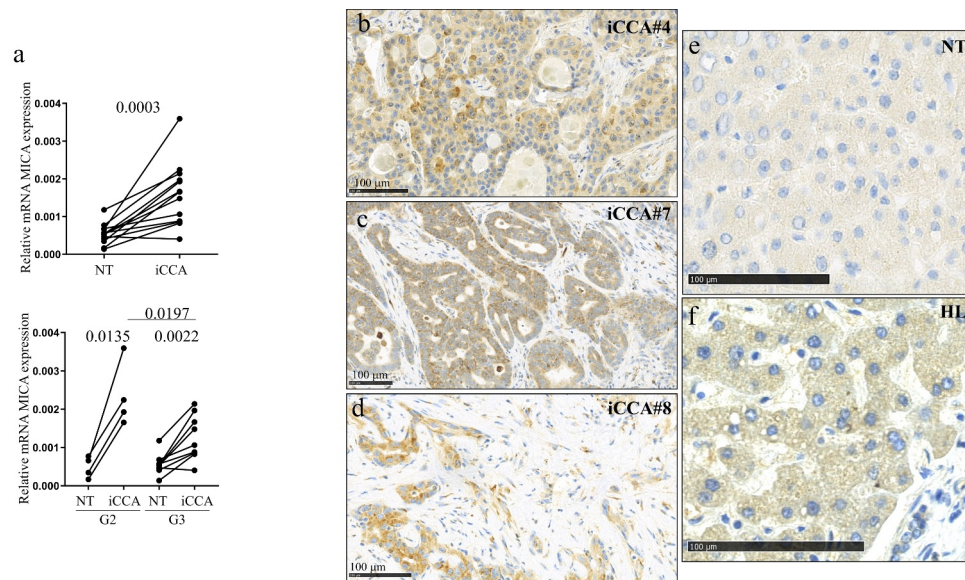
## Results

### MICA/B proteins are expressed in iCCA tissues

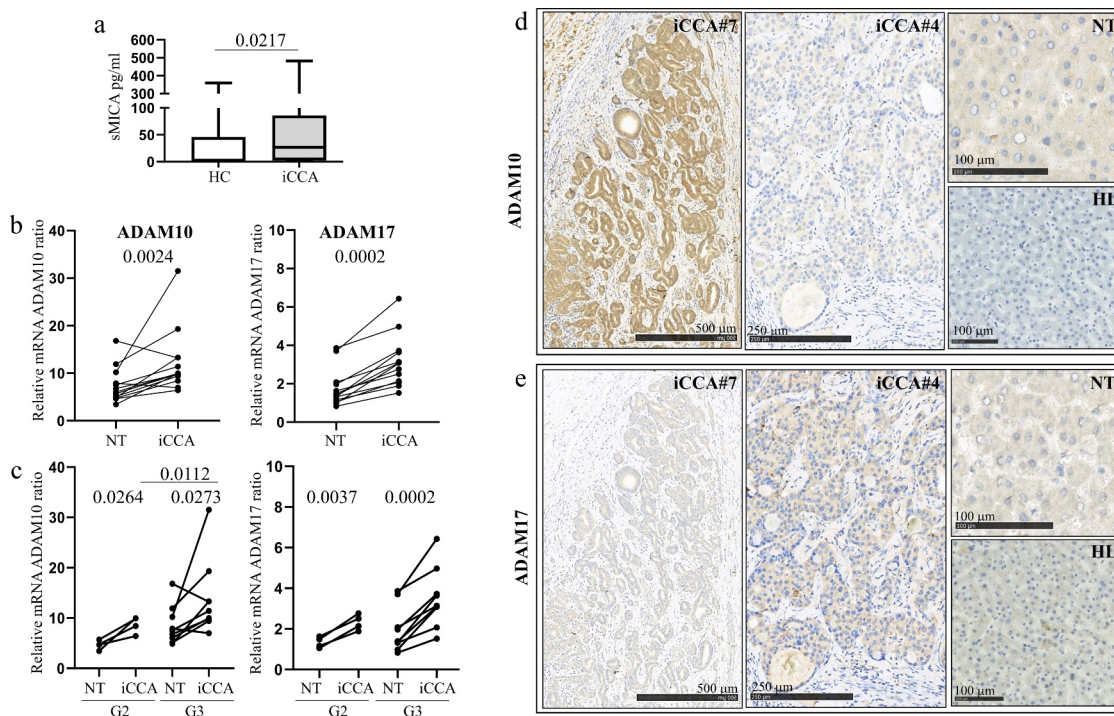
As shown in Figure 1a, MICA transcription was higher in iCCA tissue than in matched NT tissue. When MICA transcription was analyzed according to tumor grade, we observed that MICA mRNA levels were higher both in moderately-differentiated (G2) and in poorly-differentiated (G3) iCCA samples compared to matched NT. Interestingly, higher MICA mRNA levels were found in G2-iCCA tissue compared to G3-iCCA tissue (Figure 1a). We then performed immunohistochemical (IHC) analysis of MICA/B in cancer specimens from iCCA patients and matched NT tissue. All iCCA specimens available for this evaluation were classified as poorly-differentiated (G3) tumors. IHC staining revealed that MICA/B proteins were detected in all cases studied with an intensity ranging from mild to strong and a percentage of tumor parenchyma positive for IHC staining greater than 50% in all but one of the cases (Suppl. table 2). Moreover, the large majority of tumor cells (>50%) expressed MICA/B intracellularly localized likely inside vesicles as finely granular deposits, sometimes organized in rounded "globular" structures. In some cases, a membrane staining was also evident (Figure 1b-d and suppl. table 2). In most cases an intermediate staining intensity was homogeneously distributed all over the neoplastic component, compared with NT tissue. A homogeneously faint diffuse immunoreactivity and no membrane staining was observed in NT tissue and in a sample of HL tissue (Figure 1e,f).

### Serum MICA levels and tissue ADAM10/ADAM17 protease expression are elevated in iCCA patients

Since the release of MICA/B proteins by tumor cells and the concomitant increase of their soluble form are thought to represent a mechanism of immune escape evading NK immune surveillance in several neoplastic settings<sup>38,39</sup> including HCC,<sup>27,40</sup> we measured serum MICA in iCCA patients. As shown in Figure 2a, sMICA was higher in iCCA patients compared with HC. There were no significant differences in sMICA levels when iCCA patients were stratified according to etiology, tumor grading or tumor size (data not shown). Waldhauer et al.<sup>29</sup> demonstrated that ADAM10 and ADAM17 are critically involved in tumor-associated proteolytic release of sMICA. To this end, we performed a ddPCR demonstrating that mRNA expression levels of these two proteases in tumors were higher than in matched NT tissues (Figure 2b). Notably, ADAM10 transcription was higher in G3-iCCA tissue compared to G2-iCCA samples (Figure 2c). Moreover, these proteases were



**Figure 1. MICA/B proteins are expressed in iCCA tissues.** A): mRNA MICA expression on iCCA tissues along with matched NT specimens ( $n = 13$ ). Lower panel showed mRNA MICA expression in tissues stratified according to tumor grade. G2, moderately-differentiated tumor; G3, poorly-differentiated tumor. Paired and unpaired *t* tests were used to compare data. A representative immunohistochemical staining of MICA/B protein expression on iCCA tissues (b-d), NT (e) and HL specimens (f). In iCCA specimens MICA/B shows as brown cytoplasmic granules while it shows as a diffuse faint staining in NT tissues and in HL.



**Figure 2. Serum MICA levels and tissue ADAM10/ADAM17 proteases are elevated in iCCA patients** A): Serum MICA concentrations in iCCA patients ( $n = 35$ ) and HC ( $n = 46$ ). The Mann-Whitney U test was used to compare data. Middle bars represent the median values; box plots are 25% and 75% percentiles; and whiskers are minimum and maximum values. B): mRNA/ADAM10 (left panel) and mRNA/ADAM17 (right panel) ratios in iCCA tissues and in matched NT specimens ( $n = 13$ ). C): Analysis of transcription in the same tissues of panel B stratified according to tumor grade. G2, moderately-differentiated tumor ( $n = 4$ ); G3, poorly-differentiated tumor ( $n = 9$ ). The non-parametric paired Wilcoxon test and unpaired Mann-Whitney U test were used to compare data. D, E): Representative immunohistochemical staining of ADAM10 (d) and ADAM17 (e) protein expression on iCCA tissues, NT and HL specimens.

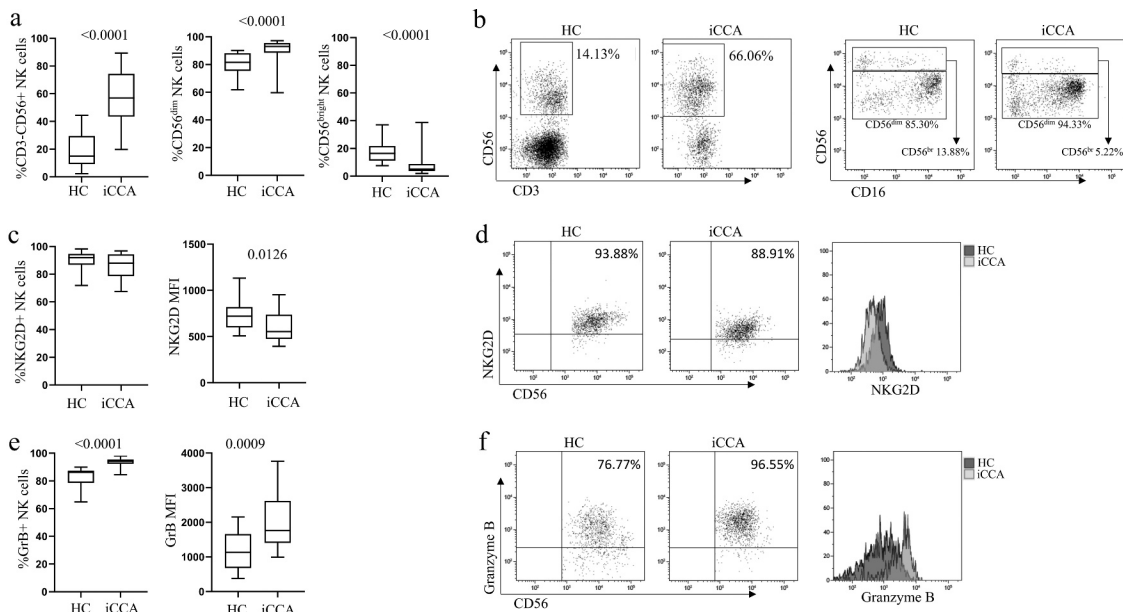
analyzed in poorly-differentiated (G3) iCCA specimens by IHC staining. ADAM10 immunoreactivity was detected in every case studied (Figure 2d and suppl. table 2), with a homogeneously diffuse and finely granular intracellular pattern, likely inside vesicles, in more than 50% of iCCA cells. NT and HL tissues

showed a very faint staining for ADAM10 (Figure 2d). ADAM17 immunoreactivity was detected as a very faint intracellular staining in >50% of cancer tissue, again likely inside vesicles, in all but one negative case (Figure 2e). NT and HL tissues showed a homogeneous faint pattern (Figure 2e).

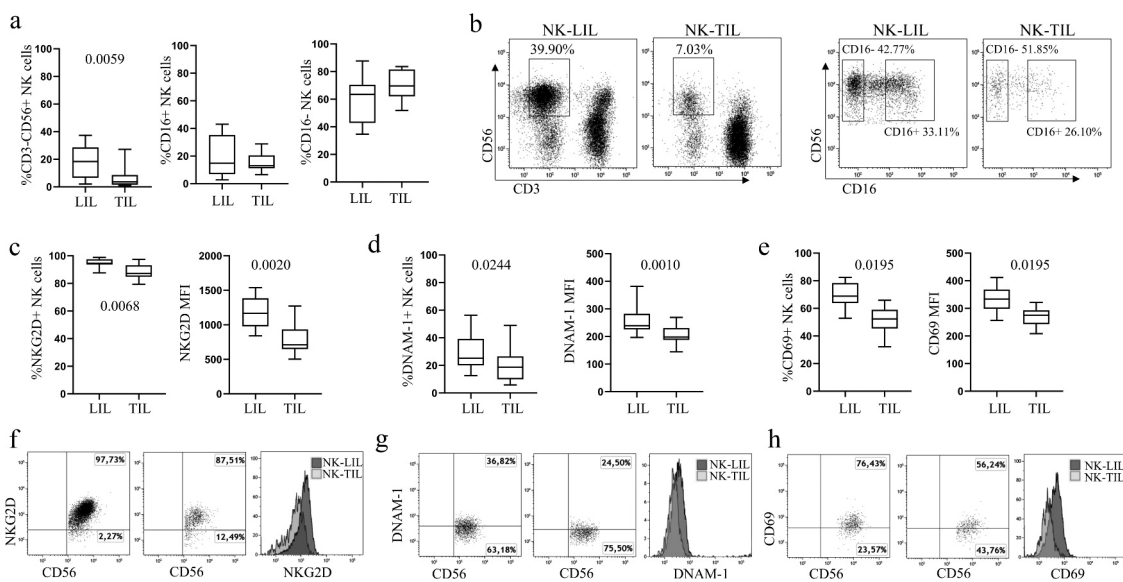
### Altered phenotype of circulating, liver- and tumor infiltrating NK cells in iCCA patients

We further analyzed the phenotype of circulating NK cells in iCCA patients and HC by flow cytometry. Supplementary figure S1A shows the gating strategy to identify NK cells and the CD56<sup>dim</sup> and CD56<sup>bright</sup> subsets. The proportion of total NK cells was significantly increased in patients compared with HC and this was accompanied by a decreased proportion of circulating T lymphocytes (Figure 3a, b and Suppl. Figure S2). Moreover, the proportion of CD56<sup>dim</sup> NK cells was significantly expanded in

iCCA patients with a concomitant reduction in the frequency of CD56<sup>bright</sup> NK cells (Figure 3a and b). We next examined the expression of the activating receptors NKG2D, NKp30, NKp46, DNAM-1 and CD16, the activation markers CD69 and TRAIL, the inhibitory receptor TIM-3 and the cytoplasmic granzyme B (GrB) granules that are responsible for NK cell cytotoxicity. Expression (Mean Fluorescence Intensity, MFI) of the NKG2D receptor on NK cells was significantly lower in patients compared with HC (Figure 3c-d). Interestingly, iCCA patients showed an increased proportion of GrB<sup>+</sup> NK cells and increased density of



**Figure 3. Circulating NK cells from iCCA patients displayed an altered frequency and phenotype.** A): frequencies of circulating CD3-CD56<sup>+</sup> NK cells, CD56<sup>dim</sup> and CD56<sup>bright</sup> subsets in iCCA patients (n = 23) and HC (n = 16). C, E): frequencies and expression (MFI) of NKG2D receptor (iCCA, n = 23; HC, n = 16) and cytotoxic GrB granules (iCCA, n = 23; HC, n = 16) on NK cells of iCCA patients and HC. The non-parametric unpaired t test was used to compare data. B, D, F): Representative dot plots and histograms of a HC and an iCCA to show NK, NKG2D and GrB distribution and expression. Middle bars represent median values; box plots are 25% and 75% percentiles; and whiskers are minimum and maximum values.



**Figure 4. Reduced expression of NKG2D, DNAM-1 and CD69 on tumor-infiltrating NK cells from iCCA patients.** A): Frequency of total CD3-CD56<sup>+</sup> NK cells and of the CD16<sup>+</sup> and CD16<sup>-</sup> subsets in LIL and TIL of iCCA patients (n = 10). Frequency and expression (MFI) of NKG2D (c), DNAM-1 (d) and CD69 (e) on LIL- and TIL-NK cell of iCCA patients. The Wilcoxon matched-pairs signed rank test was used to compare paired data. B, F, G and H): Representative dot plots of the frequency of total NKG2D<sup>+</sup>, DNAM-1<sup>+</sup> and CD69<sup>+</sup> NK cell distribution and expression (MFI) on LIL- and TIL-NK of an iCCA patient. Middle bars represent the median values; box plots are 25% and 75% percentiles; and whiskers are minimum and maximum values.



GrB on NK cells compared with HC (Figure 3e, f). There were no significant differences in other NK cell receptor expression between patients and HC (Suppl. Figure S1B-C). Stimulation with IL15 had no effect on NK phenotype with the exception of NKG2D expression that became comparable to HC (Suppl. Figures S3 and S4).

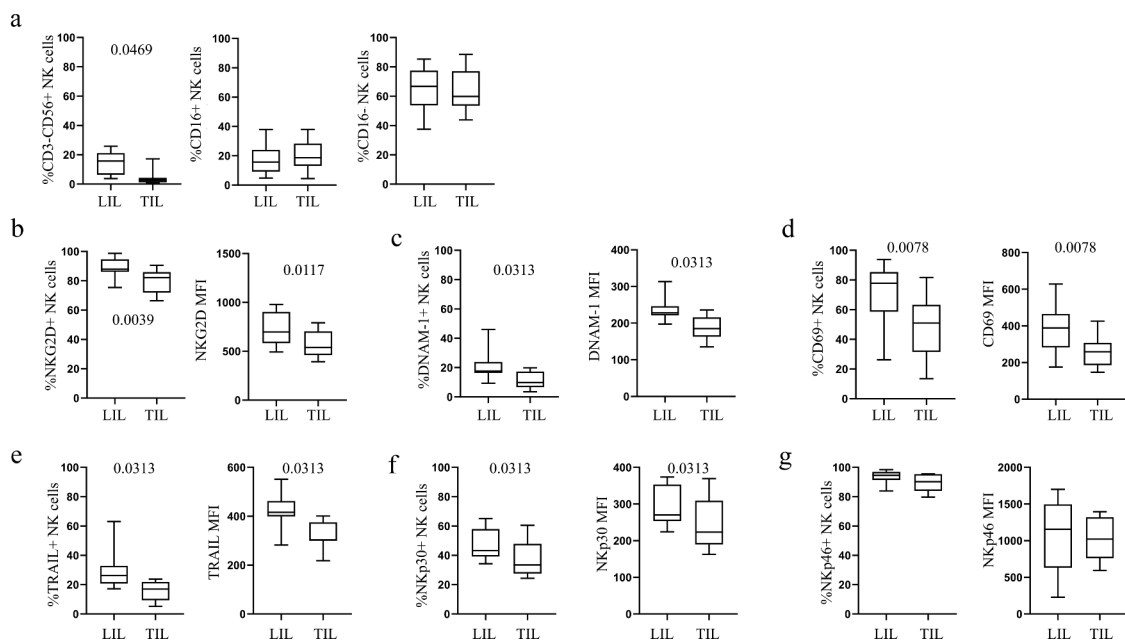
There was a decreased frequency of TIL- compared with LIL- NK cells. Moreover, the reduction of NK cells in the iCCA immune infiltrate did not result in changes in the distribution of the CD16+ and CD16- subsets (Figure 4a, b). In addition, we found a lower proportion of NK cells expressing the NKG2D and DNAM-1 activating receptors, as well as the CD69 activation molecule in TIL (Figure 4c-h). No significant differences were instead observed in CD16, GrB, TRAIL, NKp30, NKp46 and TIM-3 expression (Suppl. Figure S5). Interestingly, after IL15 stimulation, a decreased frequency of NK cells and the lower expression of NKG2D, DNAM-1 and CD69 was confirmed in TIL (Figure 5a, b, c and d). Moreover, IL15-stimulated TIL-NK also showed a lower frequency and expression of TRAIL and NKp30 molecules (Figure 5e and f). No differences were observed for NKp46 activating receptor (Figure 5g) as in unstimulated cells.

### The anti-MICA/B 7C6 mAb boosts anti-tumor function of peripheral, liver- and tumor-infiltrating NK cells from iCCA patients

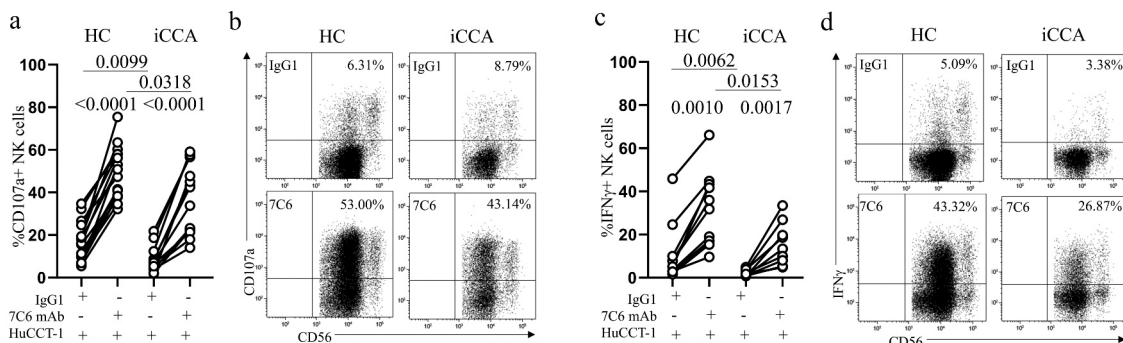
On the basis of increased MICA/B surface expression on iCCA cells, we used the 7C6 mAb to enhance NK cell-driven anti-tumor immunity.<sup>33</sup> The 7C6 mAb strongly boosted IL15 stimulated peripheral blood NK (PB-NK) cell degranulation in all individuals, compared with the IgG1 isotype control using the MICA/B-expressing HuCCT-1 cell line as target in ADCC assays (Figure 6a, b and Suppl. Figure S6). Interestingly, PB-NK cell

degranulation in iCCA patients remained lower than that of HC despite the antibody-mediated increase, suggesting reduced killing activity of iCCA PB-NK cells. Moreover, 7C6 mAb cross-linking significantly increased the proportion of IFN $\gamma$ + PB-NK cells in patients and in HC compared with isotype control, although IFN $\gamma$  production remained persistently lower in iCCA patients than in HC (Figure 6c, d). In contrast, when HC-derived highly purified NK cells were used in the ADCC assay in the presence of 7C6, there was a small, though not statistically significant, increase in the frequency of CD107a+ NK cells compared with isotype control, using HuCCT-1 cell line as the target. Interestingly, the frequency of IFN $\gamma$ + cells remained unchanged (Suppl. Figure. S7A-C). These data indicate that degranulation and IFN $\gamma$  production by NK cells after 7C6 mAb cross-linking was likely supported by interactions with as yet unidentified accessory cells. We next used primary iCCA cells derived from patient tumors, which expressed the cholangiocyte marker CK19 and MICA/B proteins (Suppl. Figure. S8), as target cells in an ADCC assay. The 7C6 mAb significantly increased degranulation of both allogeneic HC and autologous iCCA PB-NK cells (Figure 7 a, b). Of note, in the presence of 7C6, the frequency of degranulating PB-NK cells in patients became comparable to that of HC. Moreover, the mAb increased the frequency of IFN $\gamma$ + PB-NK cells both in iCCA patients and HC compared with isotype control (Figure 7c, d), even though it was persistently lower in iCCA patients than in HC.

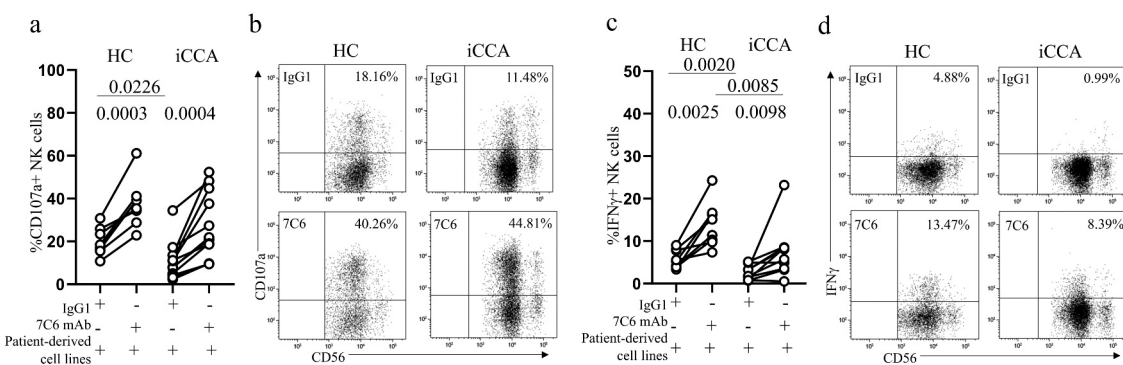
The cytotoxic potential of LIL- and TIL-NK cells for autologous primary iCCA target cells was also examined in the presence of 7C6 mAb or its isotype control. Importantly, the 7C6 mAb significantly increased degranulation of LIL-NK and of TIL-NK cells (Figure. 8a, b) although TIL-NK cells did not reach the same degranulation efficiency of LIL-NK. The frequency of IFN $\gamma$ + NK cells in LIL was higher in the presence of 7C6 mAb (Figure. 8c). Expression of ULBP proteins was sought for in HuCCT-1 and primary iCCA cells derived from



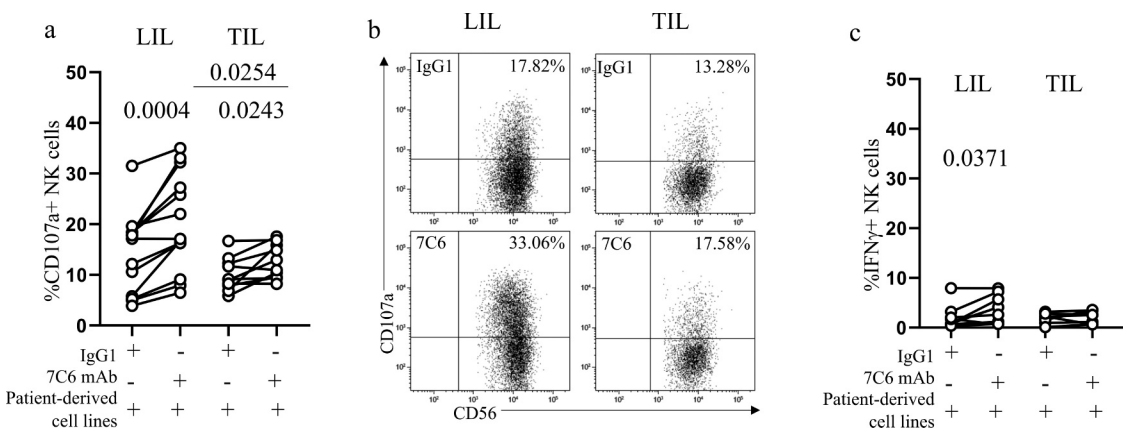
**Figure 5. Reduced expression of activating receptors on TIL-NK compared to LIL-NK after IL15 stimulation.** A) Frequency of total CD3-CD56+ NK cells and of the CD16+ and CD16- subsets on LIL and TIL from iCCA patients (n = 10). Frequency and expression (MFI) of NKG2D (b), DNAM-1 (c), CD69 (d), TRAIL (e), NKp30 (f) and NKp46 (g) on LIL- and TIL-NK cell of iCCA patients. The Wilcoxon matched-pairs signed rank test was used to compare paired data. Middle bars represent the median values; box plots are 25% and 75% percentiles; and whiskers are minimum and maximum values.



**Figure 6. Anti-MICA/B 7C6 mAb boosts anti-tumor cytotoxic function of peripheral NK cells from iCCA patients against the HuCCT-1 cell line.** A): peripheral NK cell degranulation, evaluated as frequency of CD107a+ NK cells, in iCCA patients (n = 13) and HC (n = 16) in the presence of 7C6 mAb or IgG1-Fc. Parametric paired and unpaired t tests were used to compare data. B): dot plots showing the frequency of CD3-CD56+ CD107a+ NK cells in a HC and a patient (iCCA) in the presence of 7C6 mAb or IgG1-Fc. C): the proportion of circulating IFN $\gamma$ + NK cells in patients (n = 10) and HC (n = 11) in the presence of 7C6 mAb compared with IgG1-Fc. To compare paired data, the parametric t test and the non-parametric Wilcoxon t test were used. To compare unpaired data, the parametric t test and the non-parametric Mann-Whitney U test were used. D): representative dot plots showing the frequency of CD3-CD56+ IFN $\gamma$ + NK cells in a HC and in a patient (iCCA) in the presence of 7C6 mAb or IgG1-Fc.



**Figure 7. Anti-MICA/B 7C6 mAb boosts anti-tumor cytotoxic function of peripheral NK cells from iCCA patients against patient-derived iCCA cell lines.** A): peripheral NK cell degranulation, evaluated as CD107a+ NK frequency, in iCCA patients (n = 12) and HC (n = 8) in the presence of 7C6 mAb or IgG1-Fc using patient-derived primary tumor cell lines as targets. Parametric paired and unpaired t tests were used to compare data. B): dot plots showing the frequency of CD3-CD56+ CD107a+ NK cells in a HC and in a patient (iCCA) in the presence of 7C6 mAb or IgG1-Fc. C): proportion of circulating IFN $\gamma$ + NK cells in patients (n = 10) and in HC (n = 8) in the presence of 7C6 mAb compared with IgG1-Fc. To compare paired data, we used the parametric t test and the non-parametric Wilcoxon t test. To compare unpaired data, the parametric t test and the non-parametric Mann-Whitney U test were used. D): representative dot plots showing the frequency of CD3-CD56+ IFN $\gamma$ + NK cells in a HC and in a patient (iCCA) in the presence of 7C6 mAb or IgG1-Fc.

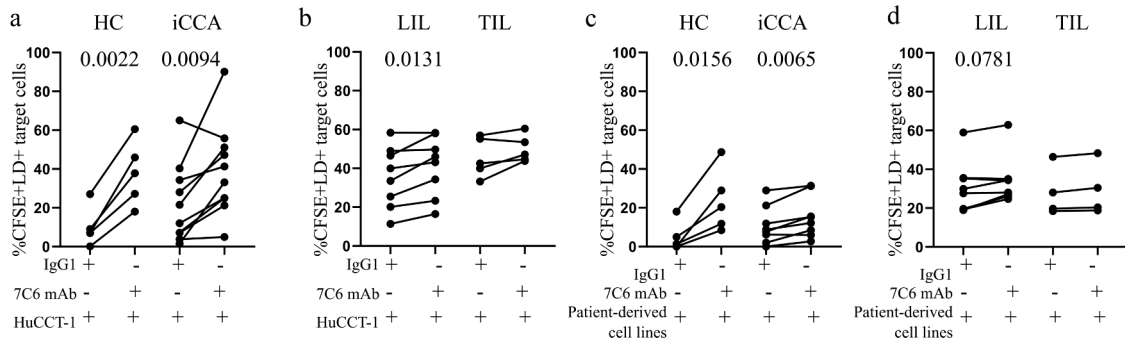


**Figure 8. 7C6 mAb enhances the anti-tumor effect of liver- and tumor-infiltrating NK cells in iCCA patients.** A): Frequency of degranulating CD107a+ NK cells in LIL (n = 13) and TIL (n = 10) of iCCA patients in the presence of anti-MICA/B 7C6 mAb or IgG1-Fc using autologous tumor-derived cell lines as targets. Parametric paired and unpaired t tests were used to compare data. B): representative dot plots showing the frequency of CD3-CD56+ CD107a+ LIL- and TIL-NK cells in the presence of 7C6 mAb or IgG1-Fc. C): proportion of IFN $\gamma$ + NK cells in LIL (n = 10) and TIL (n = 8) of iCCA patients in the presence of 7C6 mAb compared with IgG1-Fc using autologous tumor-derived cell lines as targets. The parametric t test and non-parametric Wilcoxon t test were used to compare paired data. The parametric t test was used to compare unpaired data.

patient tumors. The former did express ULBP-2/5/6 and ULBP4 proteins whereas the latter were only weakly positive for ULBP2/5/6 (Suppl. Figure. S9).

We then performed cytotoxicity assays in all conditions. 7C6 induced a higher HuCCT-1 cell death compared with isotype control when HC PBMC, patient PBMC and LIL were used as





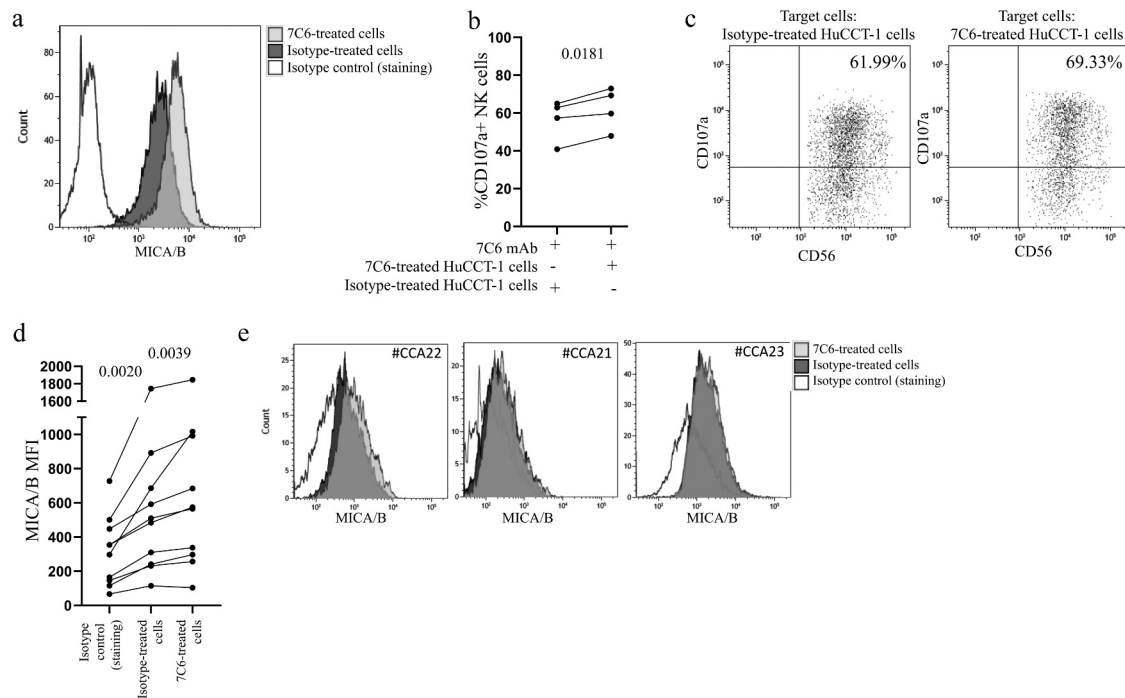
**Figure 9. Cytotoxicity assay of HC PBMC, patient PBMC, LIL and TIL cells.** A, B): Frequency of CFSE+LIVE/DEAD (LD)+ HuCCT-1 cell line targets when HC PBMC (n = 5), patient PBMC (n = 10), LIL (n = 8) and TIL (n = 5) were used as effector cells in the presence of 7C6 mAb and isotype control (IgG1). The parametric paired t tests were used to compare data. C, D): Frequency of CFSE+LD+ patient-derived cell line targets when HC PBMC (n = 5), patient PBMC (n = 8), LIL (n = 8) and TIL (n = 4) were used as effectors in the presence of 7C6 and isotype control. The parametric paired t test was used to compare data in panel C. The non-parametric Wilcoxon t test was used to compare paired data in panel D. Target cell death was determined as frequency of CFSE+LD+ cells.

effectors (Figure 9a and b). When autologous tumor cells were used as targets, patient PBMC induced a higher target cell death in the presence of 7C6 compared with isotype control (Figure 9c). LIL showed only a trend toward increased target cell death (Figure 9d), whereas TIL were largely ineffective (Figure 9b and d). In an allogeneic setting, HC-derived PBMC induced a significant increase in patient-derived tumor cell death in the presence of 7C6 (Figure 9c).

#### Increased MICA/B expression on tumor cells after 7C6 mAb treatment

Since 7C6 mAb binds the MICA/B  $\alpha 3$  domain preventing loss of cell surface MICA/B by human cancer cells,<sup>34</sup> we tested whether 7C6 mAb would also inhibit shedding in the iCCA setting. In line with evidence from other tumors,<sup>33,36</sup> MICA/B

expression increased after treatment of HuCCT-1 cells with 7C6 (Figure 10a). We then asked whether such increase could be associated with enhanced spontaneous NK cell degranulation and IFN $\gamma$  production, mediated by activating receptors such as NKG2D, in the absence of Fc receptor engagement. To this end, we used a mutated form of 7C6 to pretreat HuCCT-1 cells. This mAb carries two mutations [aspartate to alanine at position 265 (D265A) and asparagine to alanine at position 297 (N297A)] to abrogate binding to the Fc receptor but retains the ability to bind MICA/B and to inhibit MICA/B shedding to the same extent as the nonmutated form.<sup>33</sup> HuCCT-1 cells pretreated with mutant 7C6 mAb for 48 h had more MICA/B protein on the cell surface than isotype-treated cells, as assessed by flow cytometry (Suppl. Figure S10A). Spontaneous NK cell degranulation and IFN $\gamma$



**Figure 10. Increased MICA/B expression on tumor cells after 7C6 mAb pretreatment.** A): MICA/B expression on HuCCT-1 cells after treatment with 7C6 mAb and isotype control. B): frequency of CD107a+ NK cells from HC in the presence of 7C6 mAb using 7C6- and isotype-pretreated HuCCT-1 cells as target. The parametric paired t tests were used to compare data. C): representative dot plots showing the frequency of CD3-CD56+ CD107a+ NK cells shown in panel b. D): MICA/B expression (MFI) on patient-derived tumor cell lines (n = 10) after treatment with 7C6 mAb and isotype control. The non-parametric Wilcoxon t test was used to compare data. E): representative histograms showing MICA/B expression on patient-derived tumor cell lines illustrated in panel D.

production remained unchanged despite increased MICA/B expression on targets, as shown in supplementary figure S10B-C. Increased expression of MICA/B is therefore insufficient to augment the frequency of CD107a+ NK cells and of IFN $\gamma$ + NK cells in the absence of Fc receptor engagement. We next asked whether the 7C6-induced increase in MICA/B expression could improve NK cell degranulation mediated by Fc receptor engagement. When classical 7C6 mAb was used to pretreat cells for the ADCC assay, we observed a higher degranulation ability in the presence of 7C6-pretreated HuCCT-1 cells compared with isotype-treated cells (Figure 10b-c), suggesting that MICA/B enhancement was sufficient to increment degranulation after Fc receptor engagement. Moreover, patient-derived CCA cell lines treated with 7C6 mAb to inhibit MICA/B shedding showed a higher, even though variable, MICA/B expression compared with isotype-treated cells (Figure 10d-e).

## Discussion

Immunotherapy has been firmly established as a new milestone for cancer therapy, with advancements in anti-tumor treatments with monoclonal antibodies targeting immune checkpoint molecules and the development of multiple immune cells as therapeutic tools. Growing evidence in human cancer suggests that NK cell frequency, infiltration and activation status improve patient survival<sup>41-44</sup> and that NK cells are also essential for successful therapies with ICI in melanoma, head and neck squamous cell carcinoma and non-small-cell lung cancer.<sup>42,45-48</sup> Preclinical models demonstrated that solid tumors responding to ICI contained significantly more IFN $\gamma$ -producing NK cells than non-responding tumors and, in contrast, that NK cell depletion ablated ICI responses.<sup>46</sup> Although NK cells share many characteristics with CD8+ T cells, the target of current ICI therapies, they possess the unique feature to early detect and kill transformed cells that do not depend on neo-antigen presentation through MHC-I, opening to their usage to treat tumors with a very low mutational burden and those that lack neo-antigen presentation. Moreover, recent key discoveries in NK cell biology led to the identification of potent 'checkpoints' for NK cell activation that could be exploited for immunotherapy strategies aimed at synergizing with current ICI, such as IL15-driven activation,<sup>49</sup> TGF $\beta$  blockade<sup>50</sup> and CTLA-4 and PD-1 inhibitors.<sup>51</sup> To date, specifically designed immune therapies, such as ICI therapies, for iCCA are very limited, since the majority of the studies comprised all types of CCA and often gallbladder cancer. In this landscape, immunotherapeutic approaches including ICI and agents harnessing NK cell properties could be of great interest for the next wave of cancer immunotherapies.

NK cells play a key role in tumor immunosurveillance controlling metastatic dissemination, as they are abundant in the periphery. Interestingly, an inverse correlation between high amounts of circulating or TIL-NK cells and the presence of metastases at clinical presentation has been demonstrated in patients with gastrointestinal sarcoma, as well as gastric, colorectal, renal, and prostate carcinomas.<sup>52</sup> Of note, our data showed elevated frequencies of circulating NK cells in iCCA patients. Zhou et al.<sup>53</sup> demonstrated that the CCA tumor

microenvironment prevents penetration of cytotoxic immune cells but not of Tregs into the tumors. Therefore, CCA apparently belongs to the category of immune-excluded tumors in which most immune cells are sequestered at the tumor margin, pointing to potential therapeutic approaches to contrast metastasis dissemination by harnessing NK cells, for instance employing mAbs to trigger target-cell killing. The 7C6 mAb could be a powerful booster for peripheral NK responses and it could be used to increase the immunosurveillance for metastatic disease. Indeed, the iCCA microenvironment has multiple immunosuppressive elements that can promote tumor cell survival and therapeutic resistance.<sup>54</sup> In the liver context, although most NK cells display low activating receptor expression contributing to impaired functional responses, we showed that 7C6 plus IL15 could improve TIL-NK cell degranulation. In this scenario we might envisage a synergistic approach based on 7C6-mediated TIL-NK cell responses associated with co-engagement of the conserved Nkp46 receptor, as elegantly shown by others.<sup>55</sup>

The expression of NKG2D ligands, such as MICA/B, is induced in response to various stressors, including transformation, and render stressed cells susceptible to killing by cytotoxic cells.<sup>18-27</sup>

MICA/B protein expression was extensively investigated in several cancers including HCC,<sup>21</sup> but it was poorly investigated in CCA. To date, only Tsukagoshi et al.<sup>28</sup> analyzed extracellular CCA specimens for NKG2D ligand expression by immunohistochemical staining, demonstrating that almost all specimens studied expressed MICA/B proteins, that were significantly associated with overall and disease-free survival. In the present study, immunohistochemical and transcriptional analyses revealed that in iCCA tissues MICA/B proteins were also expressed. At the transcriptional level, MICA mRNA was higher in patients with G2 tumor tissues than in those expressing a G3 tumor grade. Moreover, we found that the known metzincin proteases involved in MICA shedding, ADAM10 and ADAM17, were actively transcribed in iCCA tissue and that G3 tissues displayed higher ADAM10 mRNA levels than G2 tissues. ADAM10 and ADAM17 were previously found to be upregulated in pCCA and, notably, ADAM17 was considered an independent prognostic marker for these patients.<sup>56</sup> Overall, poorly-differentiated iCCA tissue displayed low MICA transcription and high ADAM10 expression making them potentially less taggable for NKG2D-mediated NK cell cytotoxicity thereby contributing to evasion from anti-tumor immunity. We previously demonstrated elevated sMICA levels in sera from HCC patients, which stratified according to tumor grade.<sup>27</sup> Even though sMICA was also elevated in the setting of iCCA, it was not possible to reveal differences according to tumor grade.

NK cells mediate their cytotoxic function against tumors through direct cytotoxicity and ADCC.<sup>57</sup> Recently, Ferrari de Andrade et al.<sup>33</sup> produced an innovative anti-MICA/B 7C6 mAb that possesses the dual role of inhibiting MICA/B cleavage, allowing NKG2D-dependent activation of NK cell effectors and, in addition, to mediate ADCC by NK cells via engagement of the Fc $\gamma$ RIII. Moreover, Wu et al.<sup>36</sup> showed greater degranulation and IFN $\gamma$  production against different tumor cells, when 7C6 mAb was employed in combination with cytokine-induced killer cells.

In keeping with these studies and with our own data showing elevated frequencies of circulating NK cells in iCCA patients compared with HC, we showed that patients' NK cells possessed higher concentrations of lytic granules, and that tumor cells did express MICA/B, providing ground for anti-MICA/B specific antibody to strongly enhance NK degranulation and IFN $\gamma$  production. Notably, enhanced effector function was demonstrated toward an established iCCA cell line and autologous MICA/B-expressing patient-derived cell lines. Furthermore, the treatment with the unique 7C6 mAb induced a higher MICA/B expression on iCCA tumor cell line making it more taggable by NK cells in ADCC assay.

Zhou et al.<sup>53</sup> observed lower proportions of cytotoxic T cells, NK cells and increased regulatory T cells by immunohistochemistry in iCCA tumors. Notably, reduced frequencies of NKG2D+ NK cells have been observed by our group in HCC<sup>27</sup> and by others in non-hepatic tumors.<sup>32,58</sup> Here we showed that NKG2D activating receptor expression was indeed reduced in PBMC and tumor-infiltrating NK cells making them potentially unsuitable for optimal engagement of MICA/B proteins expressed on tumor cells. On the other hand, Fc $\gamma$ RIII was equally expressed on LIL- and TIL-NK cells, suggesting that TIL-NK cells could also be effective in mediating ADCC after engagement by 7C6. Moreover, circulating NK cells in iCCA patients displayed similar Fc $\gamma$ RIII expression levels compared to HC, which may identify them as a tool to control metastasis dissemination via MICA/B-directed ADCC.

Although the data have not been confirmed in animal models our findings provide preclinical evidence in support of 7C6 mAb as a potential immunotherapeutic tool for iCCA.

## Abbreviations

iCCA, intrahepatic cholangiocarcinoma; perihilar cholangiocarcinoma, pCCA; dCCA, distal cholangiocarcinoma; BTC, biliary tract cancer; PBMC, peripheral blood mononuclear cells; HC, healthy controls; NK, natural killer; HCC, hepatocellular carcinoma; NT, non-tumoral; qPCR, quantitative real-time polymerase chain reaction; ddPCR, digital droplet PCR; LIL, liver-infiltrating lymphocytes; TIL, tumor-infiltrating lymphocytes; ELISA, enzyme-linked immunosorbent assay; Tim-3, T-cell immunoglobulin and mucin-domain containing-3; NKG2D, natural killer group 2 member d; MICA/B, MHC class I chain-related molecules (MIC)A/B; ULBP1-6, cytomegalovirus UL-16 protein; IFN $\gamma$ , interferon gamma; sMICA, soluble MICA; ADCC, antibody-dependent cellular cytotoxicity; mAb, monoclonal antibody; CK19, cytokeratin 19; IHC, immunohistochemical; HL, human adult normal liver; GrB, granzyme B; ICI, immune checkpoint inhibitors; ERp5, endoplasmic reticulum protein 5; MFI, Mean Fluorescence Intensity; CFSE, carboxyfluorescein succinimidyl ester.

## Authors' contributions

SM and BO provided substantial contribution to the conception and design of the study, acquisition, analysis and interpretation of data. MUM provided substantial contribution to the conception, the design of the study, interpretation of data and revised the manuscript critically for important intellectual content. SV, DM and GrP contributed to acquisition, analysis, validation and interpretation of data; MF and DT performed immunohistochemical analysis; GT and EO analyzed clinical data and were in charge of patient care. CS, BF and RM collected and processed patient biological material. MD, GaP, MB and MM provided surgical specimens for establishment of primary

tumor cell lines and intrahepatic lymphocytes during curative surgery; SB provided samples from healthy donors. MD, GaP, MB, MM and SB also analyzed and interpreted clinical data. All analyzed and interpreted clinical data and were responsible for data curation. MUM, SM and BO supervised the team, obtained funding and had leadership responsibility for research activity planning and execution. KWW provided a unique anti-MICA/B monoclonal antibody. All authors critically read, edited and approved the final version of the manuscript.


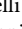
## Disclosure statement

No potential conflicts of interest were disclosed.

## Funding

This work was supported by the Ministero della Salute [08071219]. This work was supported by the Italian Ministry of Health, Ricerca Corrente [08071219 to SM]. The authors declare that this study received additional funding support from Mr. Maurizio Traglio, Enzo Cattaneo and Alberto Borella. The funders were not involved in the study design, collection, analysis, interpretation of data, the writing of this article or the decision to submit it for publication.

## ORCID

Barbara Oliviero  <http://orcid.org/0000-0002-0532-4608>  
 Stefania Varchetta  <http://orcid.org/0000-0002-0289-2896>  
 Dalila Mele  <http://orcid.org/0000-0002-5217-2766>  
 Greta Pessino  <http://orcid.org/0000-0001-6504-9882>  
 Roberta Maiello  <http://orcid.org/0000-0002-9883-4534>  
 Cristiana Soldani  <http://orcid.org/0000-0001-5041-9588>  
 Gaetano Piccolo  <http://orcid.org/0000-0002-4942-7705>  
 Matteo Barabino  <http://orcid.org/0000-0001-9525-9063>  
 Enrico Opocher  <http://orcid.org/0000-0001-5668-3136>  
 Marcello Maestri  <http://orcid.org/0000-0002-5693-9151>  
 Stefano Bernuzzi  <http://orcid.org/0000-0002-5195-6390>  
 Mario U. Mondelli  <http://orcid.org/0000-0003-1811-3153>  
 Stefania Mantovani  <http://orcid.org/0000-0002-5885-2842>

## References

- Banales JM, Marin JJG, Lamarca A, Rodrigues PM, Khan SA, Roberts LR, Cardinale V, Carpino G, Andersen JB, Braconi C, et al. Cholangiocarcinoma 2020: the next horizon in mechanisms and management. *Nat Rev Gastroenterol Hepatol.* 2020;17(9):557–588. doi:10.1038/s41575-020-0310-z.
- Khan SA, Tavolari S, Brandi G. Cholangiocarcinoma: epidemiology and risk factors. *Liver Int.* 2019;39(Suppl 1):19–31. doi:10.1111/liv.14095.
- Florio AA, Ferlay J, Znaor A, Ruggieri D, Alvarez CS, Laversanne M, Bray F, McGlynn KA, Petrick JL. Global trends in intrahepatic and extrahepatic cholangiocarcinoma incidence from 1993 to 2012. *Cancer.* 2020;126(11):2666–2678. doi:10.1002/cncr.32803.
- Fornier A, Vidili G, Rengo M, Bujanda L, Ponz-Sarvisé M, Lamarca A. Clinical presentation, diagnosis and staging of cholangiocarcinoma. *Liver Int.* 2019;39(Suppl 1):98–107. doi:10.1111/liv.14086.
- Valle J, Wasan H, Palmer DH, Cunningham D, Anthony A, Maraveyas A, Madhusudan S, Iveson T, Hughes S, Pereira SP, et al. Cisplatin plus gemcitabine versus gemcitabine for biliary tract cancer. *N Engl J Med.* 2010;362(14):1273–1281. doi:10.1056/NEJMoa0908721.
- Adeva J, Sangro B, Salati M, Edeline J, La Casta A, Bittoni A, Berardi R, Bruix J, Valle JW. Medical treatment for cholangiocarcinoma. *Liver Int.* 2019;39(Suppl 1):123–142. doi:10.1111/liv.14100.



7. Piha-Paul SA, Oh DY, Ueno M, Malka D, Chung HC, Nagrial A, Kelley RK, Ros W, Italiano A, Nakagawa K, et al. Efficacy and safety of pembrolizumab for the treatment of advanced biliary cancer: results from the KEYNOTE-158 KEYNOTE-158 and KEYNOTE-028 KEYNOTE-028 studies. *Int J Cancer*. 2020;147(8):2190–2198. doi:10.1002/ijc.33013.
8. Kim RD, Chung V, Alese OB, El-Rayes BF, Li D, Al-Toubah TE, Schell MJ, Zhou J-M, Mahipal A, Kim BH, et al. A phase 2 multi-institutional study of nivolumab for patients with advanced refractory biliary tract cancer. *JAMA Oncol*. 2020;6(6):888–894. doi:10.1001/jamaoncol.2020.0930.
9. Ueno M, Ikeda M, Morizane C, Kobayashi S, Ohno I, Kondo S, Okano N, Kimura K, Asada S, Namba Y, et al. Nivolumab alone or in combination with cisplatin plus gemcitabine in Japanese patients with unresectable or recurrent biliary tract cancer: a non-randomised, multicentre, open-label, phase 1 study. *Lancet Gastroenterol Hepatol*. 2019;4(8):611–621. doi:10.1016/S2468-1253(19)30086-X.
10. Yao W-Y, Gong W. Immunotherapy in cholangiocarcinoma: from concept to clinical trials. *Surgery in Practice and Science*. 2021 June;5:100028. doi:10.1016/j.sipas.2021.100028.
11. Feng K, Liu Y, Zhao Y, Yang Q, Dong L, Liu J, Li X, Zhao Z, Mei Q, Han W, et al. Efficacy and biomarker analysis of nivolumab plus gemcitabine and cisplatin in patients with unresectable or metastatic biliary tract cancers: results from a phase II study. *J Immunother Cancer*. 2020;8(1):e000367. doi:10.1136/jitc-2019-000367.
12. Arkenau HT, Martin-Liberal J, Calvo E, Penel N, Krebs MG, Herbst RS, Walgren RA, Widau RC, Mi G, Jin J, et al. Ramucirumab plus pembrolizumab in patients with previously treated advanced or metastatic biliary tract cancer: nonrandomized, open-label, phase i trial (JVDF). *Oncologist*. 2018;23(12):1407–e136. doi:10.1634/theoncologist.2018-0044.
13. Lin J, Yang X, Long J, Zhao S, Mao J, Wang D, Bai Y, Bian J, Zhang L, Yang X, et al. Pembrolizumab combined with lenvatinib as non-first-line therapy in patients with refractory biliary tract carcinoma. *Hepatobiliary Surg Nutr*. 2020;9(4):414–424. doi:10.21037/hbsn-20-338.
14. Guo Y, Feng K, Liu Y, Wu Z, Dai H, Yang Q, Wang Y, Jia H, Han W. Phase I study of chimeric antigen receptor-modified T cells in patients with EGFR-positive advanced biliary tract cancers. *Clin Cancer Res*. 2018;24(6):1277–1286. doi:10.1158/1078-0432.CCR-17-0432.
15. Cantoni C, Wurzer H, Thomas C, Vitale M. Escape of tumor cells from the NK cell cytotoxic activity. *J Leukoc Biol*. 2020;108(4):1339–1360. doi:10.1002/JLB.2MR0820-652R.
16. Lanier LL. NKG2D receptor and its ligands in host defense. *Cancer Immunol Res*. 2015;3(6):575–582. doi:10.1158/2326-6066.CIR-15-0098.
17. Sutherland CL, Chalupny NJ, Cosman D. The UL16-binding proteins, a novel family of MHC class I-related ligands for NKG2D, activate natural killer cell functions. *Immunol Rev*. 2001;181:185–192. doi:10.1034/j.1600-065X.2001.1810115.x.
18. Salih HR, Antropius H, Gieseke F, Lutz SZ, Kanz L, Rammensee H-G, Steinle A. Functional expression and release of ligands for the activating immunoreceptor NKG2D in leukemia. *Blood*. 2003;102(4):1389–1396. doi:10.1182/blood-2003-01-0019.
19. McGilvray RW, Eagle RA, Watson NF, Al-Attar A, Ball G, Jafferji I, Trowsdale J, Durrant LG. NKG2D ligand expression in human colorectal cancer reveals associations with prognosis and evidence for immunoeediting. *Clin Cancer Res*. 2009;15(22):6993–7002. doi:10.1158/1078-0432.CCR-09-0991.
20. McGilvray RW, Eagle RA, Rolland P, Jafferji I, Trowsdale J, Durrant LG. ULBP2 and RAET1E NKG2D ligands are independent predictors of poor prognosis in ovarian cancer patients. *Int J Cancer*. 2010;127(6):1412–1420. doi:10.1002/ijc.25156.
21. Cho H, Chung JY, Kim S, Braunschweig T, Kang TH, Kim J, Chung EJ, Hewitt SM, Kim J-H. MICA/B and ULBP1 NKG2D ligands are independent predictors of good prognosis in cervical cancer. *BMC Cancer*. 2014;14:957. doi:10.1186/1471-2407-14-957.
22. de Kruijf EM, Sajat A, van Nes JG, Putter H, Smit VT, Eagle RA, Jafferji I, Trowsdale J, Liefers GJ, van de Velde CJ, et al. NKG2D ligand tumor expression and association with clinical outcome in early breast cancer patients: an observational study. *BMC Cancer*. 2012;12:24. doi:10.1186/1471-2407-12-24.
23. Chang YT, Wu CC, Shyr YM, Chen T-C, Hwang T-L, Yeh T-S, Chang K-P, Liu H-P, Liu Y-L, Tsai M-H, et al. Secretome-based identification of ULBP2 as a novel serum marker for pancreatic cancer detection. *PLoS One*. 2011;6(5):e20029. doi:10.1371/journal.pone.0020029.
24. Paschen A, Sucker A, Hill B, Moll I, Zapatka M, Nguyen XD, Sim GC, Gutmann I, Hassel J, Becker JC, et al. Differential clinical significance of individual NKG2D ligands in melanoma: soluble ULBP2 as an indicator of poor prognosis superior to S100B. *Clin Cancer Res*. 2009;15(16):5208–5215. doi:10.1158/1078-0432.CCR-09-0886.
25. Vetter CS, Groh V, Thor Straten P, Spies T, Bröcker EB, Becker JC. Expression of stress-induced MHC class I related chain molecules on human melanoma. *J Invest Dermatol*. 2002;118(4):600–605. doi:10.1046/j.1523-1747.2002.01700.x.
26. Kamei R, Yoshimura K, Yoshino S, Inoue M, Asao T, Fuse M, Wada S, Kuramasu A, Furuya-Kondo T, Oga A, et al. Expression levels of UL16 binding protein 1 and natural killer group 2 member D affect overall survival in patients with gastric cancer following gastrectomy. *Oncol Lett*. 2018;15(1):747–754. doi:10.3892/ol.2017.7354.
27. Mantovani S, Varchetta S, Mele D, Donadon M, Torzilli G, Soldani C, Franceschini B, Porta C, Chiellino S, Pedrazzoli P, et al. An anti-MICA/B antibody and IL-15 rescue altered NKG2D-dependent NK cell responses in hepatocellular carcinoma. *Cancers (Basel)*. 2020;12(12):3583. doi:10.3390/cancers12123583.
28. Tsukagoshi M, Wada S, Yokobori T, Altan B, Ishii N, Watanabe A, Kubo N, Saito F, Araki K, Suzuki H, et al. Overexpression of natural killer group 2 member D ligands predicts favorable prognosis in cholangiocarcinoma. *Cancer Sci*. 2016;107(2):116–122. doi:10.1111/cas.12853.
29. Waldhauer I, Goehlsdorf D, Gieseke F, Weinschenk T, Wittenbrink M, Ludwig A, Stevanovic S, Rammensee H-G, Steinle A. Tumor-associated MICA is shed by ADAM proteases. *Cancer Res*. 2008;68(15):6368–6376. doi:10.1158/0008-5472.CAN-07-6768.
30. Liu G, Atteridge CL, Wang X, Lundgren AD, Wu JD. The membrane type matrix metalloproteinase MMP14 mediates constitutive shedding of MHC class I chain-related molecule A independent of A disintegrin and metalloproteinases. *J Immunol*. 2010;184:3346–3350. doi:10.4049/jimmunol.0903789.
31. Salih HR, Rammensee HG, Steinle A. Cutting edge: down-regulation of MICA on human tumors by proteolytic shedding. *J Immunol*. 2002;169(8):4098–4102. doi:10.4049/jimmunol.169.8.4098.
32. Groh V, Wu J, Yee C, Spies T. Tumor-derived soluble MIC ligands impair expression of NKG2D and T-cell activation. *Nature*. 2002;419(6908):734–738. doi:10.1038/nature01112.
33. Ferrari de Andrade L, Tay RE, Pan D, Luoma AM, Ito Y, Badrinath S, Tsoucas D, Franz B, May KF, Harvey CJ, et al. Antibody-mediated inhibition of MICA and MICB shedding promotes NK cell-driven tumor immunity. *Science*. 2018;359(6383):1537–1542. doi:10.1126/science.aao0505.
34. Ferrari de Andrade L, Kumar S, Luoma AM, Ito Y, Alves da Silva PH, Pan D, Pyrdol JW, Yoon CH, Wucherpennig KW. Inhibition of MICA and MICB shedding elicits NK-cell-mediated immunity against tumors resistant to cytotoxic T cells. *Cancer Immunol Res*. 2020;8(6):769–780. doi:10.1158/2326-6066.CIR-19-0483.
35. Alves da Silva PH, Xing S, Kotini AG, Papapetrou, EP, Song X, Wucherpennig, KW, Mascarenhas, J, Ferrari de Andrade, L, et al. MICA/B antibody induces macrophage-mediated immunity against acute myeloid leukemia [published online ahead of print, 2021 Aug 6]. *Blood* 139 2 205–216 . 2021; blood.2021011619.
36. Wu X, Zhang Y, Li Y, Schmidt-Wolf IGH. Increase of antitumoral effects of cytokine-induced killer cells by antibody-mediated inhibition of MICA shedding. *Cancers (Basel)*. 2020;12(7):1818. doi:10.3390/cancers12071818.

37. Mantovani S, Oliviero B, Lombardi A, Varchetta S, Mele D, Sangiovanni A, Rossi G, Donadon M, Torzilli G, Soldani C, et al. Deficient natural killer cell Nkp30-mediated function and altered NCR3 splice variants in hepatocellular carcinoma. *Hepatology*. 2019;69(3):1165. doi:10.1002/hep.30235.
38. Hilpert J, Grosse-Hovest L, Grünebach F, Buechele C, Nuebling T, Raum T, Steinle A, Salih HR. Comprehensive analysis of NKG2D ligand expression and release in leukemia: implications for NKG2D-mediated NK cell responses. *J Immunol*. 2012;189(3):1360–1371. doi:10.4049/jimmunol.1200796.
39. Jinushi M, Vanneman M, Munshi NC, Tai Y-T, Prabhala RH, Ritz J, Neuberg D, Anderson KC, Carrasco DR, Dranoff G, et al. MHC class I chain-related protein A antibodies and shedding are associated with the progression of multiple myeloma. *Proc Natl Acad Sci U S A*. 2008;105(4):1285–1290. doi:10.1073/pnas.0711293105.
40. Kumar V, Yi Lo PH, Sawai H, Kato N, Takahashi A, Deng Z, Urabe Y, Mbarek H, Tokunaga K, Tanaka Y, et al. Soluble MICA and a MICA variation as possible prognostic biomarkers for HBV-induced hepatocellular carcinoma. *PLoS One*. 2012;7(9):e44743. doi:10.1371/journal.pone.0044743.
41. Cursons J, Souza-Fonseca-Guimaraes F, Foroutan M, Anderson A, Hollande F, Hediye-Zadeh S, Behren A, Huntington ND, Davis MJ. A gene signature predicting natural killer cell infiltration and improved survival in melanoma patients. *Cancer Immunol Res*. 2019;7(7):1162–1174. doi:10.1158/2326-6066.CIR-18-0500.
42. Lee H, Quek C, Silva I, Tasker A, Batten M, Rizos H, Lim SY, Nur Gide T, Shang P, Attrill GH, et al. Integrated molecular and immunophenotypic analysis of NK cells in anti-PD-1 treated metastatic melanoma patients. *Oncoimmunology*. 2018;8(2):e1537581. 31. doi:10.1080/2162402X.2018.1537581.
43. Li B, Jiang Y, Li G, Fisher GA Jr, Li R. Natural killer cell and stroma abundance are independently prognostic and predict gastric cancer chemotherapy benefit. *JCI Insight*. 2020;5(9):e136570. doi:10.1172/jci.insight.136570.
44. Gil M, Kim KE. Interleukin-18 is a prognostic biomarker correlated with CD8<sup>+</sup> T cell and natural killer cell infiltration in skin cutaneous melanoma. *J Clin Med*. 2019;8(11):1993. doi:10.3390/jcm81110.3390/jcm8111993. PMID: 31731729; PMCID: PMC6912818.
45. Barry KC, Hsu J, Broz ML, Cueto FJ, Binnewies M, Combes AJ, Nelson AE, Loo K, Kumar R, Rosenblum MD, et al. A natural killer-dendritic cell axis defines checkpoint therapy-responsive tumor microenvironments. *Nat Med*. 2018;24(8):1178–1191. doi:10.1038/s41591-018-0085-8.
46. Zemek RM, De Jong E, Chin WL, Schuster IS, Fear VS, Casey TH, Forbes C, Dart SJ, Leslie C, Zaitouny A, et al. Sensitization to immune checkpoint blockade through activation of a STAT1/NK axis in the tumor microenvironment. *Sci Transl Med*. 2019;11(501):eaav7816. doi:10.1126/scitranslmed.aav7816.
47. Prat A, Navarro A, Paré L, Reguart N, Galván P, Pascual T, Martínez A, Nuciforo P, Comerma L, and Alos L, et al. Immune-related gene expression profiling after PD-1 blockade in non-small cell lung carcinoma, head and neck squamous cell carcinoma, and melanoma. *Cancer Res*. 2017;77(13):3540–3550. doi:10.1158/0008-5472.CAN-16-3556.
48. Mazzaschi G, Facchinetti F, Missale G, Canetti D, Madeddu D, Zecca A, Veneziani M, Gelsomino F, Goldoni M, Buti S, et al. The circulating pool of functionally competent NK and CD8<sup>+</sup> cells predicts the outcome of anti-PD1 treatment in advanced NSCLC. *Lung Cancer*. 2019;127:153–163. doi:10.1016/j.lungcan.2018.11.038.
49. Easom NJW, Stegmann KA, Swadling L, Pallett LJ, Burton AR, Odera D, Schmidt N, Huang W-C, Fusai G, Davidson B, et al. IL-15 overcomes hepatocellular carcinoma-induced NK cell dysfunction. *Front Immunol*. 2018;9(9):1009. doi:10.3389/fimmu.2018.01009.
50. Gao Y, Souza-Fonseca-Guimaraes F, Bald T, Ng SS, Young A, Ngiow SF, Rautela J, Straube J, Waddell N, Blake SJ, et al. Tumor immunoevasion by the conversion of effector NK cells into type 1 innate lymphoid cells. *Nat Immunol*. 2017;18(9):1004–1015. doi:10.1038/ni.3800.
51. Khan M, Arooj S, Wang H. NK cell-based immune checkpoint inhibition. *Front Immunol*. 2020;11:167. doi:10.3389/fimmu.2020.00167.
52. López-Soto A, Gonzalez S, Smyth MJ, Galluzzi L. Control of metastasis by NK cells. *Cancer Cell*. 2017;32(2):135–154. doi:10.1016/j.ccell.2017.06.009.
53. Zhou G, Sprengers D, Mancham S, Erkens R, Boor PPC, van Beek AA, Doukas M, Noordam L, Campos Carrascosa L, de Ruiter V, et al. Reduction of immunosuppressive tumor microenvironment in cholangiocarcinoma by ex vivo targeting immune checkpoint molecules. *J Hepatol*. 2019;71(4):753–762. doi:10.1016/j.jhep.2019.05.026.
54. Fabris L, Sato K, Alpini G, Strazzabosco M. The tumor microenvironment in cholangiocarcinoma progression. *Hepatology*. 2021;73(Suppl 1):75–85. doi:10.1002/hep.31410.
55. Gauthier L, Morel A, Anceriz N, Rossi B, Blanchard-Alvarez A, Grondin G, Trichard S, Cesari C, Sapet M, Bosco F, et al. Multifunctional natural killer cell engagers targeting Nkp46 trigger protective tumor immunity. *Cell*. 2019;177(7):1701–1713.e16. doi:10.1016/j.cell.2019.04.041.
56. Jiao X, Yu W, Qian J, Chen Y, Wei P, Fang W, Yu G. ADAM-17 is a poor prognostic indicator for patients with hilar cholangiocarcinoma and is regulated by FoxM1. *BMC Cancer*. 2018;18:570. doi:10.1186/s12885-018-4294-9.
57. Wang W, Erbe AK, Hank JA, Morris ZS, Sondel PM. NK cell-mediated antibody-dependent cellular cytotoxicity in cancer immunotherapy. *Front Immunol*. 2015;6:368. doi:10.3389/fimmu.2015.00368.
58. Lee JC, Lee KM, Kim DW, Heo DS. Elevated TGF-beta1 secretion and down-modulation of NKG2D underlies impaired NK cytotoxicity in cancer patients. *J Immunol*. 2004;172(12):7335–7340. doi:10.4049/jimmunol.172.12.7335.